Translational Oncology
www.transonc.com

Volume 6 Number 6 December 2013 pp. 676–684 676

EV20, a Novel Anti–ErbB-3 Humanized Antibody, Promotes ErbB-3 Down-Regulation and Inhibits Tumor Growth *In Vivo*[1]

Gianluca Sala*,†, Ilario Giovanni Rapposelli†, Reza Ghasemi†,‡, Enza Piccolo*,†, Sara Traini*,†, Emily Capone†, Cosmo Rossi†, Angela Pelliccia§, Annalisa Di Risio*,†, Maurizia D'Egidio†, Nicola Tinari*,†, Raffaella Muraro*,†, Stefano Iacobelli*,† and on behalf of Consorzio Interuniversitario Nazionale per la Bio-Oncologia (CINBO)

*MediaPharma srl, Chieti, Italy; †Department of Experimental and Clinical Sciences, G. D'Annunzio University Foundation, Chieti, Italy; ‡Department of Medical Genetics, School of Medicine, Tehran University of Medical Sciences (TUMS), Tehran, Iran; §Sigma-Tau Industrie Farmaceutiche Riunite SpA, Pomezia, Italy

Abstract

ErbB-3 (HER-3) receptor is involved in tumor progression and resistance to therapy. Development of specific inhibitors impairing the activity of ErbB-3 is an attractive tool for cancer therapeutics. MP-RM-1, a murine monoclonal antibody targeting human ErbB-3, has shown anticancer activity in preclinical models. With the aim to provide novel candidates for clinical use, we have successfully generated a humanized version of MP-RM-1. The humanized antibody, named EV20, abrogates both ligand-dependent and ligand-independent receptor signaling of several tumor cell types, strongly promotes ErbB-3 down-regulation, and efficiently and rapidly internalizes into tumor cells. Furthermore, treatment with EV20 significantly inhibits growth of xenografts originating from prostatic, ovarian, and pancreatic cancers as well as melanoma in nude mice. In conclusion, we provide a novel candidate for ErbB-3–targeted cancer therapy.

Translational Oncology (2013) 6, 676–684

Introduction

ErbB-3 (HER-3) is one of the four members of the epidermal growth factor receptor (or ErbB) family. These receptors transduce extracellular signals into the cell, which strictly regulate key cellular processes such as proliferation, survival, migration, and invasion. Abnormal ErbB activity has been reported in several human cancers and is considered a hallmark of malignancy [1–5]. As a consequence, ErbB-1 and ErbB-2 receptors are the most targeted oncoproteins in cancer [6,7].

Although ErbB-3 has significantly reduced kinase activity when compared to other members of the family [8], its activity has been documented in several cancers, including breast, lung, prostate, pancreas, ovary, and head and neck cancers as well as melanoma [9–15]. ErbB-3 is unique in that it is able to potently activate downstream phosphatidylinositol-3-kinase (PI3K) through six consensus phosphotyrosine sites, not present on ErbB-1 and ErbB-2 [16]. Activated PI3K results in the recruitment and activation of Akt, a master regulator of downstream pathways that are implicated in a plethora of processes critical for tumorigenesis and therapy resistance [17]. Indeed, most tumors require PI3K/Akt signaling for their survival, which is often achieved by an abnormally hyperactive upstream receptor ErbB-3 [18].

Therefore, an increasing attention is directed to ErbB-3 as a target for cancer therapy, documented by the fact that many ErbB-3 inhibitors, i.e., monoclonal antibodies (mAbs), are currently under clinical development [19–21].

We have recently developed a murine mAb, named MP-RM-1, that specifically recognizes the extracellular domain (ECD) of ErbB-3 [22]. This antibody has been shown to possess strong antitumoral activity both *in vitro* and *in vivo* through the disruption of the ErbB-3/Akt

Address all correspondence to: Dr Gianluca Sala, Center of Excellence for Aging Sciences, G. D'Annunzio University Foundation, Via Colle dell'Ara 1, 66100 Chieti, Italy.
E-mail: g.sala@unich.it

[1]This article refers to supplementary materials, which are designated by Figures W1 and W2 and are available online at www.transonc.com.

Received 17 June 2013; Revised 27 September 2013; Accepted 30 September 2013

DOI 10.1593/tlo.13475

signaling pathway, suggesting that MP-RM-1 may represent an excellent candidate for targeted therapy in tumors with activated ErbB-3 [22]. Therefore, in an attempt to develop an agent endowed with a potential anti-cancer clinical application, we have generated 4 chimeric and 16 humanized variants of MP-RM-1 and selected the humanized variant EV20 as the lead compound. Here, we describe the ability of EV20 to target ErbB-3, downregulate its activity, and internalize it into tumor cells. Furthermore, we demonstrate that EV20 can inhibit the growth of several tumor xenografts in nude mice.

Materials and Methods

Antibody Humanization and Chimerization

MP-RM-1 chimeric variants were generated by fusing the variable domain of the heavy chain and the variable domain of the light chain of the murine antibody to the corresponding human constant domains. Four variants were generated using IgG1 and IgG3 heavy chain (HC) subtypes and κ and λ light chain (LC) subtypes. Humanized MP-RM-1 variants were generated by identifying murine complementary determinant regions (CDRs) that were grafted onto a human antibody framework. The IgG1 isotype was used for all humanized variants. Libraries of human antibodies were screened to identify the optimal human framework for the HC and LC. In defining the optimal framework, long continuous stretches of human sequence in any given framework region were identified. The HC and LC human frameworks are based on the accession number sequences CAB37147 and AAX82494, respectively. Sixteen humanized antibody variants were constructed by replacing selected residues in the human framework with their MP-RM-1 counterparts. Recombinant genes were placed into the pCDNA3.1 expression vector and transfected into Chinese Hamster Ovary-S cells. For small/medium-scale production of antibody variants, transiently transfected Chinese Hamster Ovary-S cells were grown using a benchtop BioFlo 3000 bioreactor (New Brunswick Scientific, Enfield, CT); antibody-containing supernatants were purified by ultrafiltration (VivaFlow-200 membrane; Sartorius Stedim Biotech, Goettingen, Germany) and immune selection on a Protein-A (Pall Protein A ceramic HyperD F) affinity matrix. EV20 affinity was determined by surface plasmon resonance assays as described [23].

Reagents

Antibodies were given as follows: phosphorylated ErbB-3 (Tyr^{1289}), phosphorylated Akt (Ser^{473}), and Akt from Cell Signaling Technology (Danvers, MA); C-17 ErbB-3 from Santa Cruz Biotechnology (Santa Cruz, CA); anti-actin, rhodamine-labeled phalloidin, and protein synthesis inhibitor CHX were purchased from Sigma-Aldrich Corporation (St Louis, MO). Neuregulin-1β (NRG-1β) and recombinant human ECD ErbB-3/Fc chimera were purchased from R&D Systems, Inc (Minneapolis, MN). Recombinant human ECD ErbB-3 was from ACROBiosystems (Bethesda, MD). F(ab′)2 preparation kit was purchased from Pierce (Thermo Fisher Scientific, Inc, Rockford, IL).

Cell Culture

DU-145 (prostate), Fadu (head and neck), BxPC-3 (pancreas), MDA-MB-435 (melanoma), Skbr-3, and MDA-MB-361 (breast) human cancer cells were purchased from American Type Culture Collection (Rockville, MD); OVCAR-8 (ovary) cells were from National Cancer Institute/National Institutes of Health (NCI/NIH; Frederick, MD). The human melanoma cell line IR-8 [24] was kindly provided by Dr Carlo Leonetti ("Regina Elena" NCI, Rome, Italy). The gastric carcinoma cell line MKN-45 [25] was kindly provided by Dr Sergio Anastasi ("Regina Elena" NCI). IR-8 4Mut and IR-8 shErbB-3 cells were generated as described [22,26]. All cell lines were grown in RPMI 1640 or Dulbecco's modified Eagle's medium (Invitrogen, Carlsbad, CA) supplemented with 10% heat-inactivated FBS (Invitrogen), L-glutamine, and antibiotics (Sigma-Aldrich Corporation) and incubated in 5% CO_2 at 37°C.

Immunoblot Analysis

Lysates from cells in culture were prepared by washing cells twice in cold phosphate-buffered saline (PBS) followed by lysis with either HNTG buffer [50 mM Hepes (pH 7.5), 150 mM NaCl, 10% glycerol, 1% Triton X-100, and 5 mM EGTA] or RIPA lysis buffer supplemented with protease and phosphatase inhibitors (Sigma-Aldrich Corporation). Immunoblot analysis was performed as described [22]. Western blot (WB) bands were densitometrically quantified using ImageJ software. To study ErbB-2/ErbB-3 heterodimerization, immunoprecipitation assays were performed using the anti–ErbB-2 antibody trastuzumab covalently linked to AminoLink Coupling Resin (Pierce). Linking of the antibody to the resin was performed overnight at 4°C.

FACS Assays

For ErbB-3 surface expression analysis, cells were incubated on ice in the presence of 1 μg/ml EV20 for 0.5 hour and then returned to 37°C for 1 hour, harvested, and stained with an Alexa Fluor 488 goat anti-human antibody (Molecular Probes, Life Technologies, Paisley, United Kingdom). Alternatively, cells were exposed to increasing doses of EV20 for 6 hours at 37°C, detached, and incubated with 100 nM of anti–ErbB-3 (MAB 3481 from R&D Systems, Inc) for 30 minutes at 4°C, followed by Alexa Fluor specific secondary antibodies (Molecular Probes, Life Technologies). The murine ErbB-3 antibody MAB 3481 does not interfere with EV20 for ErbB-3 binding (data not shown). After labeling, samples were analyzed by flow cytometry using a FACS Calibur cytometer (Becton Dickinson, Buccinasco, Italy). Data analysis to quantify changes in the mean surface receptor fluorescence values was performed as described [27].

Confocal Microscopy

IR-8 cells grown on coverslips were treated as follows: 1) cells were incubated with EV20 on ice for 1 hour to induce binding of the antibody to the plasma membrane; 2) cells were incubated for different lengths of time with EV20 together with LysoTracker Red (1 hour) at 37°C to analyze antibody internalization. Cells were then fixed in 4% paraformaldehyde for 15 minutes at room temperature, permeabilized with 0.25% Triton X-100 for 5 minutes, and blocked with 0.1% BSA for 1 hour at room temperature. Coverslips were then incubated for 2 hours at room temperature with the indicated primary antibodies, followed by Alexa Fluor specific secondary antibodies (Molecular Probes, Life Technologies). DRAQ5 (Vinci-Biochem, Firenze, Italy) was used to visualize nuclei. Images were acquired with a Zeiss LSM 510 meta-confocal microscope (Zeiss, Oberkochen, Germany) using 488-, 543-, and 633-nm lasers. Quantification of co-localization was performed with WCiF ImageJ software, using a co-localization plug-in.

Soft-Agar Colony Formation Assay

For the anchorage-independent growth assay with IR-8, BxPC-3, DU-145, and MKN-45 cell lines, 3×10^4 cells were plated per well in 12-well plates. The assay was then performed as described [22].

Table 1. Screening of MP-RM-1 Variants.

Antibody Variant	Inhibitory Effect (Long-Term)	Inhibitory Effect (Short-Term)	Down-Regulation	K_d (nM)
cMP-RM-1 #1	+++	++++	+++	1.35
cMP-RM-1 #2	+++	+	++	–
cMP-RM-1 #3	+++	+	++	–
cMP-RM-1 #4	++++	+/–	+	–
hMP-RM-1 #5	+++	++	+	–
hMP-RM-1 #6	+++	++++	+++	1.74
hMP-RM-1 #7	+++	++++	++	–
hMP-RM-1 #8	+++	++++	++	–
hMP-RM-1 #9	+++	++++	++	–
hMP-RM-1 #10	+++	++++	+++	1.16
hMP-RM-1 #11	+++	++++	++	–
hMP-RM-1 #12	+++	++++	++	–
hMP-RM-1 #13	+++	++	++	–
hMP-RM-1 #14	++++	++	++	–
hMP-RM-1 #15	+++	++	++	–
hMP-RM-1 #16	+++	+	++	–
hMP-RM-1 #17	++++	++	++	–
hMP-RM-1 #18	+++	++	+	–
hMP-RM-1 #19	+++	++++	++	–
hMP-RM-1 #20	++++	++++	+++	1.30

Inhibitory effect (long-term) refers to the inhibition of ErbB-3/Akt phosphorylation in serum-starved (24-hour) IR-8 cells incubated with the antibody variants for 2 hours and then stimulated with NRG-1β for 5 minutes. Inhibitory effect (short-term) refers to the inhibition of ErbB-3/Akt phosphorylation in serum-starved (24-hour) IR-8 cells co-exposed to antibody variants and NRG-1β for 5 minutes. Down-regulation refers to the ability of the antibody variants to promote ErbB-3 down-regulation in IR-8 cells as evaluated by WB and FACS. K_d is determined by surface plasmon resonance. Antibody isotype is IgG3 for cMP-RM-1 #3 and cMP-RM-1 #4 and IgG1 for all other variants.

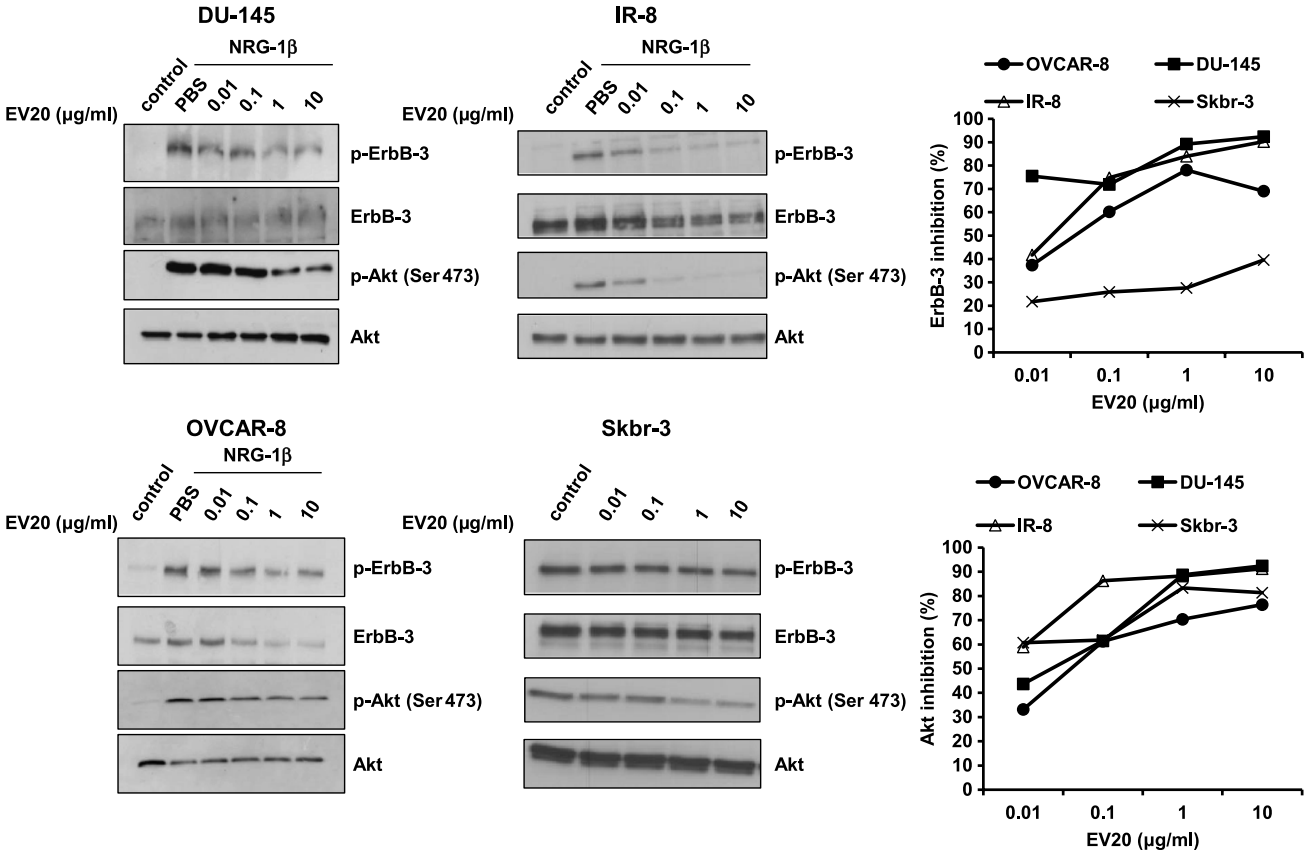

Figure 1. EV20 inhibits ErbB-3/Akt activation in both a ligand-dependent and a ligand-independent manner. To study the effect of EV20 on ligand-dependent activation of ErbB-3/Akt, DU-145, IR-8, and OVCAR-8 cells were serum starved for 24 hours and then treated with increasing doses of EV20 for 2 hours, before stimulation with 10 ng/ml NRG-1β (5 minutes). For ligand-independent assay, the serum-starved (24-hour) Skbr-3 cells were treated with increasing doses of the antibody for 2 hours and then harvested. Lysates obtained from cells were immunoblotted as indicated. Immunoreactivity was quantified and plotted after normalization to total Akt. Data are presented as percentage of inhibition of ErbB-3/Akt phosphorylation in EV20-treated samples over control. The presented data are representative of two independent experiments.

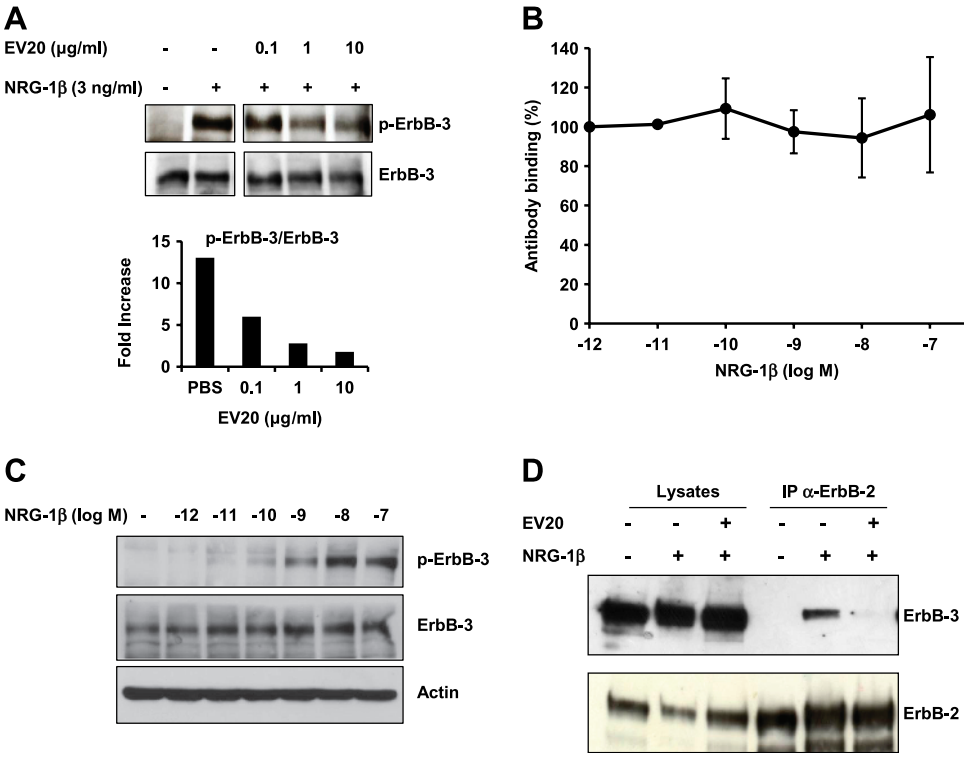

Figure 2. EV20 inhibits ErbB-2/ErbB-3 dimerization without competing with NRG-1β for binding to ErbB-3. (A) MDA-MB-361 cells were co-exposed to 3 ng/ml NRG-1β and increasing doses of EV20 for 10 minutes. Anti–p-ErbB-3 immunoreactivity was quantified and plotted after normalization to total ErbB-3. The data are representative of two independent experiments. (B) For FACS, MDA-MB-435 cells were incubated on ice with increasing concentrations of NRG-1β for 1 hour, then with 0.15 μg/ml EV20 (concentration giving 50% of maximal binding, as previously determined) for 45 minutes, and finally with the Alexa Fluor 488–conjugated anti-human secondary antibody for 30 minutes. Plotted results are an average ± SD of three independent experiments. (C) For WB, MDA-MB-435 cells were incubated for 1 hour on ice with increasing concentrations of NRG-1β. Cell lysates were probed as indicated. (D) For immunoprecipitation, MDA-MB-361 cells were treated for 30 minutes with 10 μg/ml EV20 and then stimulated for 10 minutes with 10 ng/ml NRG-1β. The lysates were immunoprecipitated for ErbB-2 and probed as indicated.

Animal Studies

Athymic CD-1 nu/nu mice (5 or 7 weeks old) were purchased from Charles River Laboratories (Calco, Italy) and maintained under specific pathogen-free conditions with food and water provided *ad libitum*. The animal health status was monitored daily. Procedures involving animals and their care were conducted according to the institutional guidelines in compliance with national and international laws and policies. Xenografts were generated by subcutaneous injection into the right flank of mice of 5×10^6 (IR-8, BxPC-3, OVCAR-8, and DU-145) or 3×10^6 (MKN-45) cells in 200 μl of PBS. When xenografts became palpable, animals were divided into two groups ($n = 10$) in a way to provide a similar range of tumor size for each group. In the case of MKN-45 xenograft, six and five mice were used for the control and treated groups, respectively. The treated group received twice weekly intraperitoneal injections of 10 mg/kg EV20 in PBS, whereas the control group received PBS only. Tumor volume was monitored every week by a caliper and calculated by the following formula: tumor volume (mm^3) = (length × width^2)/2. At the end of the study, mice were anesthetized with isoflurane inhalation before cervical dislocation. Tumors were excised and snap frozen for WB analysis as previously described [26]. For EV20 detection in serum and tumor samples, ELISA was performed as described [28], using goat anti-human IgG Fc (Jackson ImmunoResearch, Newmarket, United Kingdom) as a capture antibody and goat anti-human HRP (Jackson ImmunoResearch) as the detecting antibody.

Statistics

P values were determined by Student's *t* test and considered significant for $P < .05$ (*in vivo* xenograft experiments, co-localization assays) or $P < .001$ (soft agar assay).

Results

Antibody Screening and Lead Selection

Four chimeric and 16 humanized variants of murine MP-RM-1 antibody were generated as described in the Materials and Methods section. With the aim to identify the antibody variants with the highest activity, we carried out an initial screening where antibody efficacy was evaluated as the ability to 1) inhibit ErbB-3/Akt phosphorylation and 2) promote ErbB-3 down-regulation. Inhibition of ErbB-3/Akt phosphorylation was assessed both in a long-term assay (cells incubated with the antibody for 2 hours and then stimulated with NRG-1β for 5 minutes) and a short-term assay (cells co-exposed to antibody and NRG-1β for 5 minutes).

All the analyzed antibody variants were able to inhibit ErbB-3/Akt phosphorylation and promote receptor down-regulation. However, one chimeric (cMP-RM-1 #1) and three humanized (hMP-RM-1 #6, hMP-RM-1 #10, hMP-RM-1 #20) antibodies resulted with the best score in the screening with no significant differences in affinity

for the receptor (Table 1). Therefore, given the minor immunogenicity of humanized compared to chimeric antibodies, hMP-RM-1 #20, hereafter named EV20, was chosen as the lead compound for further development.

EV20 Inhibits Akt Activation and ErbB-2/ErbB-3 Dimerization without Competing with NRG-1β for Binding to ErbB-3

To investigate if EV20 is able to interfere with ligand-dependent and ligand-independent ErbB-3/Akt activation, a panel of cancer cell lines was treated for 2 hours with increasing doses of EV20. To study NRG-1β–driven ErbB-3 activation, we used ovarian (OVCAR-8), prostate (DU-145), and melanoma (IR-8) cells. For ligand-independent ErbB-3 activation, we used the ErbB-2–amplified breast cancer cells, Skbr-3, that possess constitutive ErbB-3 activity. As shown in Figure 1, treatment with EV20 dose dependently inhibited ErbB-3/Akt activation both in the ligand-dependent and ligand-independent models; moreover, EV20 was able to downregulate receptor levels, although to variable extents according to the cell line assayed. No effect was observed when cells were exposed to human IgG1 isotype control antibody compared to vehicle (PBS), whereas treatment with trastuzumab, a humanized IgG1 anti–ErbB-2 antibody, produced a strong inhibition of ErbB-3 and Akt phosphorylation (Figure W1*A*). Notably, the F(ab′)2 fragment retained the same activity of the full-length (FL) antibody in terms of inhibition of ErbB-3/Akt phosphorylation (Figure W1*B*).

We next studied whether EV20 could act as an antagonist for NRG-1β on ErbB-3 activation. MDA-MB-361 breast cancer cells co-exposed to 3 ng/ml NRG-1β and increasing doses of EV20 for 10 minutes showed a dose-dependent inhibition of ErbB-3 phosphorylation, therefore indicating that the antibody is able to act as a ligand antagonist

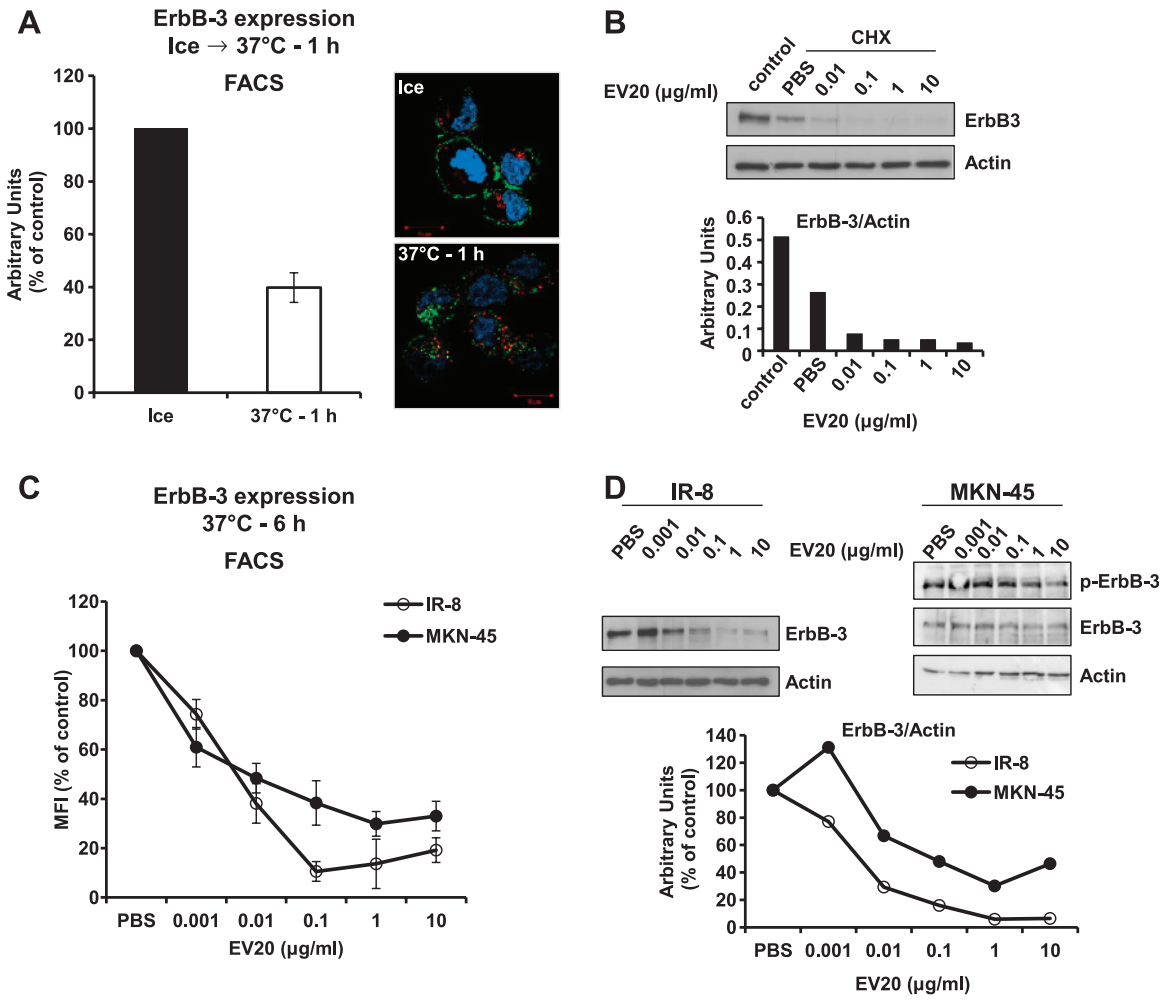

Figure 3. EV20 induces ErbB-3 down-regulation. (A) IR-8 cells were maintained for 30 minutes on ice in the presence of 10 μg/ml EV20 and placed back at 37°C for 1 hour. ErbB-3 expression and localization were evaluated by FACS (left) and by confocal microscopy imaging (right). The histogram represents the percentage of mean fluorescence intensity (MFI) referred to control (cells maintained on ice). Plotted results are an average ± SD of three independent experiments. For confocal microscopy imaging, EV20 and the early endosome marker EEA1 were visualized in green and red, respectively. Cell nuclei are shown in blue. (B) IR-8 cells were incubated for 3 hours with 10 μg/ml CHX in the presence or absence of increasing doses of EV20. Lysates were probed with the indicated antibodies. Anti–ErbB-3 immunoreactivity was quantified and plotted after normalization for actin. (C and D) IR-8 and MKN-45 cells were exposed to increasing doses of EV20 for 6 hours and then analyzed for surface and total ErbB-3 expression by FACS (C; one representative of three independent experiments is shown) and WB (D), respectively. Anti–ErbB-3 immunoreactivity was quantified and plotted after normalization for actin. The data shown in B and D are representative of two independent experiments.

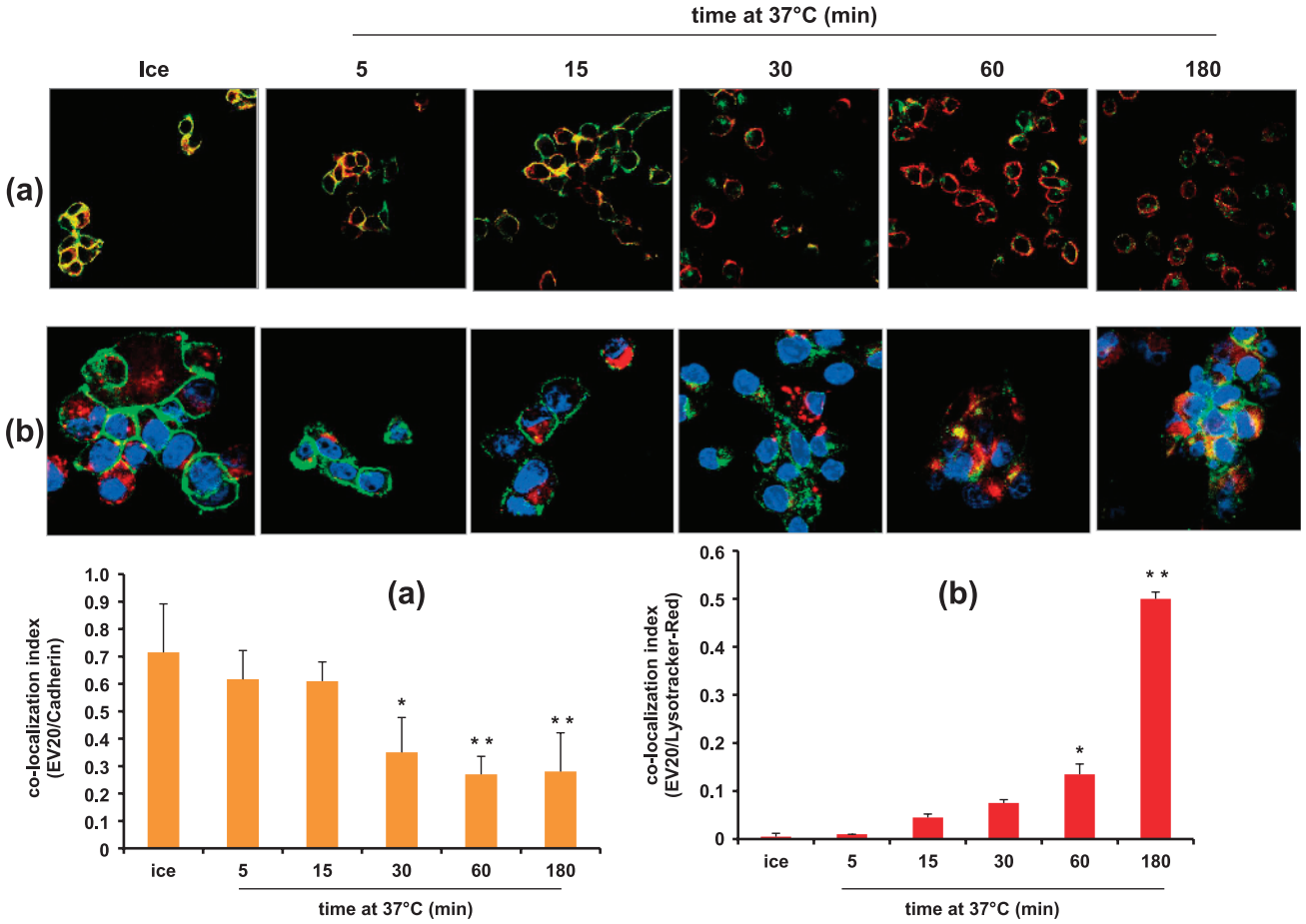

Figure 4. EV20 internalizes into IR-8 cells. IR-8 cells were maintained on ice for 1 hour or placed at 37°C for the indicated times in the presence of 10 μg/ml EV20. EV20 is visualized in green and cadherin (A) and LysoTracker Red (B) in red. Cell nuclei are shown in blue. Co-localization index values of EV20/cadherin (A) and EV20/LysoTracker Red (B) were obtained by analyzing five different fields for each point in two independent experiments and reported as means ± SD in the histograms. *$P < .05$, **$P < .01$. Bar, 10 μm.

(Figure 2*A*). Interestingly, despite these antagonizing properties of the antibody, FACS analysis demonstrated that EV20 does not compete with NRG-1β for the ligand binding site of the receptor (Figure 2*B*). As a control, phosphorylation of ErbB-3 was assessed by WB in cells stimulated with NRG-1β, under the same conditions of the FACS assay (incubation on ice; Figure 2*C*).

Having demonstrated that EV20 possesses short-term activity, we investigated whether the antibody is also able to prevent ErbB-2/ErbB-3 dimerization upon ligand stimulation. We took advantage of MDA-MB-361 cells, which endogenously express high levels of both the receptors and in which ErbB-2/ErbB-3 dimerization is inducible by the ligand. After serum starvation, cells were treated for 30 minutes with 10 μg/ml EV20, then stimulated for 10 minutes with 10 ng/ml NRG-1β following which ErbB-2/ErbB-3 dimerization was evaluated by immunoprecipitation. As illustrated, EV20 completely abolished NRG-1β–induced ErbB-2/ErbB-3 dimerization (Figure 2*D*). Taken together, these data indicate that EV20 exhibits a dual short-term and long-term activity impairing ErbB-2/ErbB-3 dimerization and downstream pathway activation.

EV20 Promotes ErbB-3 Down-Regulation

To further investigate ErbB-3 down-regulation induced by EV20, IR-8 cells were exposed to the antibody on ice for 0.5 hour, then to 37°C for 1 hour, after which ErbB-3 surface expression was analyzed by FACS. As illustrated in Figure 3*A*, surface expression of the receptor was reduced by approximately 60% in cells incubated at 37°C compared to the control group that remained on ice, suggesting receptor/antibody internalization. This was confirmed by confocal microscopy (Figure 3*A*, *right*).

Moreover, cells treated with the protein synthesis inhibitor CHX in the presence of the antibody displayed a remarkable, dose-dependent reduction of ErbB-3 expression compared to those exposed to vehicle (PBS), indicating the ability of EV20 to accelerate receptor degradation (Figure 3*B*). The same results were obtained when using the F(ab′)2 fragment instead of the FL antibody (Figure W1*C*). To estimate the "net" effect of the antibody on ErbB-3 levels, we used IR-8 and MKN-45 cells (as ligand-dependent and ligand-independent models, respectively) for a long-term (6-hour) treatment with increasing concentrations of EV20 in the presence of serum and in the absence of NRG-1β and CHX. As depicted, in both cell lines, the antibody dose-dependently reduced both the surface and total ErbB-3 expression (Figure 3, *C* and *D*, respectively). Constitutive activity of ErbB-3 in MKN-45 cells was significantly abrogated by treatment with the antibody (Figure 3*D*). The ability of EV20 to reduce ErbB-3 expression on the cell surface was confirmed in a panel of cancer cells, although with variable efficiency depending on the cell line used (Figure W1*D*).

EV20 Efficiently Internalizes into Tumor Cells

To further analyze EV20 internalization, IR-8 cells were incubated with the antibody (10 μg/ml) on ice for 1 hour or at 37°C for different times. Quantitative immunofluorescence analysis showed that cells on ice displayed a complete co-localization of signals from EV20 and cadherin at the plasma membrane, whereas, on incubation at 37°C, co-localization was reduced in a time-dependent manner, reaching a nadir after 60 minutes. In a reverse approach, cells were incubated with EV20 in the presence of LysoTracker Red to identify the lysosomal compartment. Under these conditions, a time-dependent increase in co-localization of EV20/LysoTracker Red was observed (Figure 4).

Moreover, tracking the receptor using an anti–ErbB-3 antibody that recognizes the C-terminal residue (C-17), thus not competing with EV20, resulted in the co-localization of the two antibodies, indicating that internalized EV20 was still bound to the receptor (Figure W1*E*).

The internalization is dependent on ErbB-3 expression, as neither EV20 binding to cell membrane nor intracellular localization of the antibody was seen in ErbB-3 silenced cells (Figure W2*A*), which displayed an about 80% reduction in the level of the receptor and an almost complete abrogation of ErbB-3/Akt activation (Figure W2, *B* and *C*).

EV20 Exerts Antitumor Activity In Vitro *and* In Vivo

Finally, we studied the *in vitro* and *in vivo* antitumor efficacies of EV20 by performing colony formation assays and xenograft experiments, respectively. To this end, we used a panel of cancer cell lines

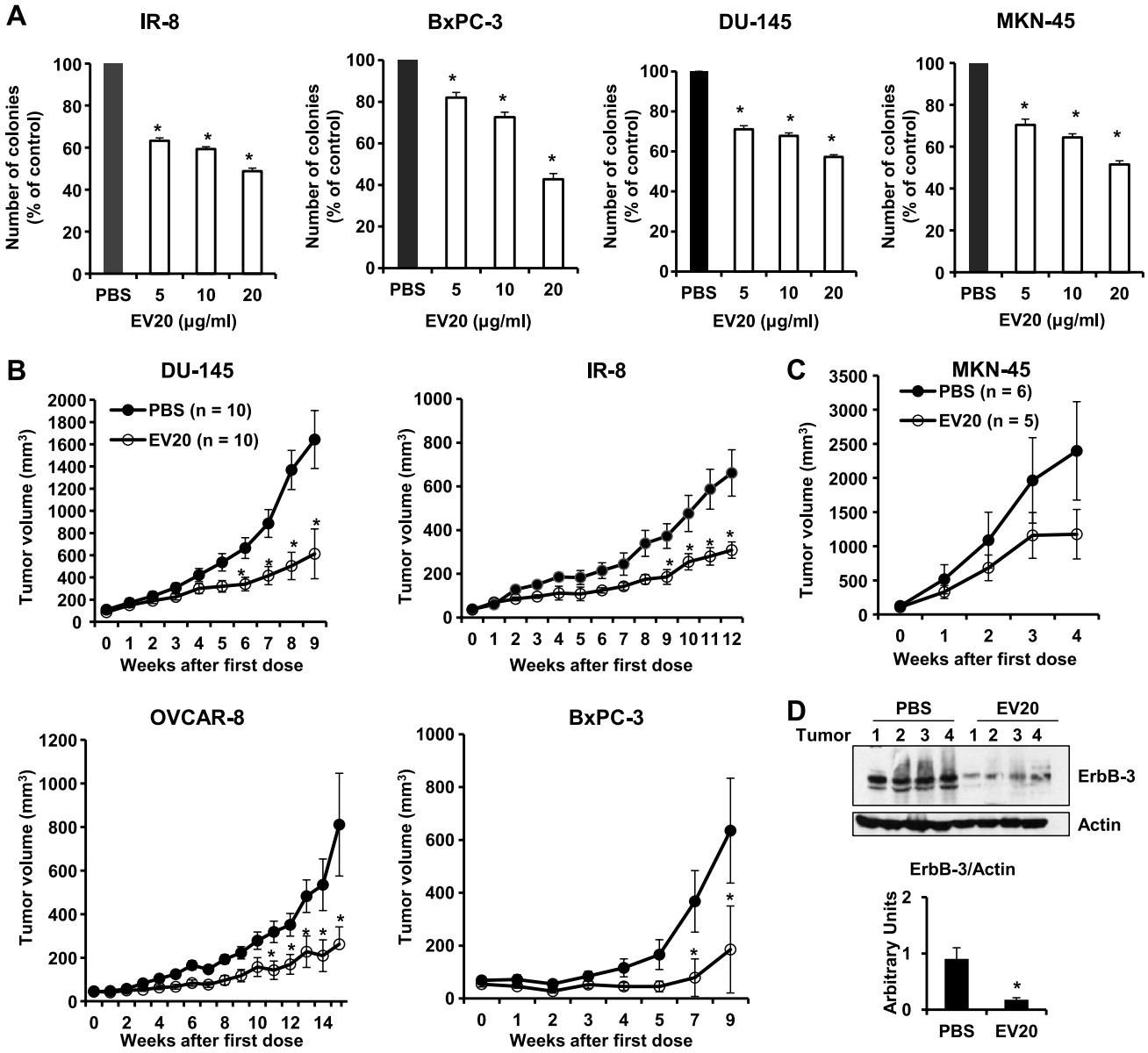

Figure 5. EV20 exerts antitumor activity *in vitro* and *in vivo*. (A) The effect of EV20 on anchorage-independent cell growth of IR-8, BxPC-3, DU-145, and MKN-45 cells was evaluated by determining the number of colonies formed in soft agar. Data are an average ± SD of three experimental replicates. *$P < .001$. (B and C) DU-145, IR-8, OVCAR-8, BxPC-3, and MKN-45 cells were injected into recipient mice. Animals were treated twice a week with 10 mg/kg EV20 or with vehicle alone (PBS). Tumor growth was assessed as described in the Materials and Methods section. *$P < .05$. (D) WB analysis of tumor lysates of OVCAR-8 xenografts excised after 6 hours of treatment with 10 mg/kg EV20 or PBS. Anti–ErbB-3 immunoreactivity was quantified and plotted after normalization to actin. *$P < .01$.

originating from different solid tumors, including gastric (MKN-45), pancreatic (BxPC-3), prostatic (DU-145), and ovarian (OVCAR-8) carcinomas and melanoma (IR-8). As shown in Figure 5*A*, EV20 dose-dependently reduced colony formation in all cell lines.

For the *in vivo* study, EV20 was administered twice a week as a single agent at the dose of 10 mg/kg. This treatment resulted in a significant reduction in tumor volume in all models studied compared to their control groups, respectively. The volume was reduced by more than 50% in DU-145 and IR-8 xenografts and by about 70% in OVCAR-8 and BxPC-3 xenografts, respectively ($P < .05$; Figure 5*B*). A similar trend, although not significant, was observed in the MKN-45 xenograft group (Figure 5*C*).

Immunoblot analysis of ErbB-3 in tumor xenografts taken from mice 6 hours after a single dose injection of 10 mg/kg EV20 revealed a marked reduction of receptor expression, indicating that EV20 is able to mediate ErbB-3 down-regulation *in vivo* (Figure 5*D*). Finally, concentrations of EV20 in tumor tissue and serum of mice taken 24 hours after the last antibody injection ranged between 110 and 130 ng/mg tissue and 540 and 740 ng/ml, respectively (Figure W2*D*).

Discussion

ErbB-3 plays a relevant role in the progression of several malignancies [3,11], and its expression is associated with a reduction in survival rates in patients affected by several different types of solid tumors [9]. Recent data have documented for the first time ErbB-3 oncogenic mutations in many cancer types but most prevalent in patients with gastric and colon cancers [29]. Additionally, ErbB-3 is involved in drug resistance in several cancer models. For example, ErbB-3 is activated by c-MET in lung cancer cells resistant to the ErbB-1 inhibitor gefitinib [30], and its overexpression has been found to be associated with resistance to ErbB-2 inhibitors in ErbB-2–amplified breast cancer and to the anti–ErbB-2 antibody pertuzumab in ovarian cancer [31]. Recently, feedback up-regulation of ErbB-3 has been described in breast cancer cells treated with PI3K inhibitors or the dual ErbB-2/ErbB-1 inhibitor lapatinib [32,33] and in melanoma cells treated with RAF/mitogen-activated protein kinase kinase (MEK) inhibitors [34].

These data indicate that ErbB-3 may represent an important therapeutic target, and as such, focus has been directed toward the development of ErbB-3 inhibitors to be used as anticancer agents in the clinical setting [19–21].

Recently, we have generated a murine mAb targeting ErbB-3, which possessed anticancer activity *in vitro* and *in vivo* [22]. However, the use of murine antibodies in humans is severely limited by the development of a human anti-murine antibody response occurring in up to 50% of patients, which compromises the safety, efficacy, and biologic half-life of these reagents [35].

Recombinant DNA technology has allowed to largely overcome human anti-murine antibody response through the chimerization or humanization of murine mAbs [36]. In this work, 4 chimeric and 16 humanized variants of the murine MP-RM-1 antibody were generated by the fusion of the MP-RM-1 variable domain of the heavy chain and variable domain of the light chain portions to the corresponding human constant domains and by grafting the CDRs LC and HC into a human framework, respectively. All variants were shown to possess antigen binding capabilities comparable to that of the parent antibody, as measured by FACS or ELISA (data not shown). These results are consistent with the fact that all the antibody variants share the same parental CDRs, only differing for selected amino acids in the framework region. Moreover, all the antibodies were able to interfere with ErbB-3/Akt activation and reduce receptor activity, although with differing efficacies. The humanized variant EV20 was selected as the lead compound.

EV20 possessed a dissociation constant (K_d) of 1.3 nM, as determined by surface plasmon resonance. Cell binding experiments, performed by FACS assay and ELISA using the ECD of human ErbB-3, confirmed that the affinity of EV20 for the receptor is in the nanomolar range (data not shown). We observed no significant variation in K_d values between the parental and humanized antibodies (0.4 and 1.3 nM, respectively), indicating that the humanization process has not significantly affected its affinity, although it should be noted that these values are substantially higher than that previously reported for the murine antibody (K_d = 32 nM) [22]. This difference is likely dependent on the type of antigen used. Indeed, in our previous analysis, ErbB-3 ECD was in a dimeric state because of a fused Fc tail, whereas, in the present analysis, ErbB-3 ECD was monomeric.

EV20 demonstrated the capacity to impair ligand-dependent and ligand-independent ErbB-3/Akt activation. Moreover, we show that this antibody is able to antagonize the NRG-1β–induced ErbB-2/ErbB-3 dimerization without competing with the ligand for binding to the receptor. Therefore, it is reasonable to speculate that EV20, once bound to ErbB-3, induces a conformational change in the receptor that, despite allowing NRG-1β binding, impairs ErbB-3 heterodimerization and phosphorylation. Identification of the epitope and critical residues for EV20 binding to ErbB-3 ECD is currently under investigation.

In addition to the short-term activity, EV20 was able to dramatically reduce ErbB-3 activity in a long-term treatment. Indeed, we were able to demonstrate that a 2- to 6-hour treatment with EV20 1) reduces ErbB-3 at the cell surface, 2) accelerates ErbB-3 degradation, and 3) reduces total ErbB-3 expression.

Another important feature of EV20 is its ability to efficiently internalize into tumor cells. Using quantitative immunofluorescence analysis, we found that more than 50% of the antibody internalized after 30 minutes and this internalization was strictly dependent on ErbB-3 expression level, as it was not evidenced in cells silenced for ErbB-3.

In vivo antitumor activity of EV20 was also assessed in this study. The antibody treatment proved to be effective in inhibiting growth of prostatic, ovarian, pancreatic tumor, and melanoma xenografts. Although not significant, possibly because of the very aggressive behavior of cells *in vivo* and of the small sample size in the experiment, similar trends were obtained with tumor xenografts from the c-MET–addicted MKN-45 gastric cancer cells. We have previously demonstrated that tumors from animals treated with the murine MP-RM-1 antibody display a significant lower cell proliferation activity *in vivo*, as measured by Ki-67 staining and cell mitotic index [22]. In this work, we confirmed that treatment with EV20 was able to strongly promote receptor down-regulation *in vivo*.

The ability of EV20 to promote receptor down-regulation makes this new antibody an attractive candidate for ErbB-3–targeted cancer therapy. In fact, recent findings underscore the notion that ErbB-3 up-regulation mediated by forkhead box transcription factors may be a general mechanism by which the cancer cells treated with targeted drugs adopt to bypass the block of signaling pathways [32–34].

While the use of naked antibodies is an interesting approach to treat patients with ErbB-3–positive cancer, the generation of an ErbB-3–based antibody–drug conjugate could also represent a substantial improvement over this immunotherapeutic approach [37]. As such,

the ability of EV20 to efficiently and rapidly internalize into ErbB-3–expressing tumor cells makes this antibody an ideal candidate for the generation of an antibody–drug conjugate with the potential of blocking tumor growth by a dual mechanism, i.e., by directly interfering with ErbB-3 signaling and by delivering drug/payload into ErbB-3–expressing tumor cells.

In conclusion, our findings demonstrate that EV20 antibody has the therapeutic potential to target and inhibit ErbB-3–dependent cancer growth in a clinical setting and therefore warrants further research and development.

Acknowledgments

We thank M. Hildinger (Evitria AG, Zurich, Switzerland) for antibody humanization, F. Petronzelli (Sigma-Tau Industrie Farmaceutiche Riunite SpA, Pomezia, Italy) for surface plasmonic resonance analysis and discussion, and A. Sala and V. De Laurenzi for discussion. G.S. give special thanks to S. Abu-Hayyeh (from Imperial College London, London, United Kingdom) for manuscript revision.

References

[1] Sharma SV and Settleman J (2009). ErbBs in lung cancer. *Exp Cell Res* **315**, 557–571.

[2] Wu WK, Tse TT, Sung JJ, Li ZJ, Yu L, and Cho CH (2009). Expression of ErbB receptors and their cognate ligands in gastric and colon cancer cell lines. *Anticancer Res* **29**, 229–234.

[3] Hynes NE and MacDonald G (2009). ErbB receptors and signaling pathways in cancer. *Curr Opin Cell Biol* **21**, 177–184.

[4] Hynes NE and Lane HA (2005). ERBB receptors and cancer: the complexity of targeted inhibitors. *Nat Rev Cancer* **5**, 341–354.

[5] Holbro T, Civenni G, and Hynes NE (2003). The ErbB receptors and their role in cancer progression. *Exp Cell Res* **284**, 99–110.

[6] Ross JS, Slodkowska EA, Symmans WF, Pusztai L, Ravdin PM, and Hortobagyi GN (2009). The HER-2 receptor and breast cancer: ten years of targeted anti–HER-2 therapy and personalized medicine. *Oncologist* **14**, 320–368.

[7] Robinson KW and Sandler AB (2013). EGFR tyrosine kinase inhibitors: difference in efficacy and resistance. *Curr Oncol Rep* **15**, 396–404.

[8] Shi F, Telesco SE, Liu Y, Radhakrishnan R, and Lemmon MA (2010). ErbB3/HER3 intracellular domain is competent to bind ATP and catalyze autophosphorylation. *Proc Natl Acad Sci USA* **107**, 7692–7697.

[9] Ocana A, Vera-Badillo F, Seruga B, Templeton A, Pandiella A, and Amir E (2012). HER3 overexpression and survival in solid tumors: a meta-analysis. *J Natl Cancer Inst* **105**, 266–273.

[10] Cook RS, Garrett JT, Sánchez V, Stanford JC, Young C, Chakrabarty A, Rinehart C, Zhang Y, Wu Y, Greenberger L, et al. (2011). ErbB3 ablation impairs PI3K/Akt-dependent mammary tumorigenesis. *Cancer Res* **71**, 3941–3951.

[11] Campbell MR, Amin D, and Moasser MM (2010). HER3 comes of age: new insights into its functions and role in signaling, tumor biology, and cancer therapy. *Clin Cancer Res* **16**, 1373–1383.

[12] Wimmer E, Kraehn-Senftleben G, and Issing WJ (2008). HER3 expression in cutaneous tumors. *Anticancer Res* **28**, 973–979.

[13] Reschke M, Mihic-Probst D, van der Horst EH, Knyazev P, Wild PJ, Hutterer M, Meyer S, Dummer R, Moch H, and Ullrich A (2008). HER3 is a determinant for poor prognosis in melanoma. *Clin Cancer Res* **14**, 5188–5197.

[14] Grivas PD, Antonacopoulou A, Tzelepi V, Sotiropoulou-Bonikou G, Kefalopoulou Z, Papavassiliou AG, and Kalofonos H (2007). HER-3 in colorectal tumourigenesis: from mRNA levels through protein status to clinicopathologic relationships. *Eur J Cancer* **43**, 2602–2611.

[15] Tanner B, Hasenclever D, Stern K, Schormann W, Bezler M, Hermes M, Brulport M, Bauer A, Schiffer IB, Gebhard S, et al. (2006). ErbB-3 predicts survival in ovarian cancer. *J Clin Oncol* **24**, 4317–4323.

[16] Prigent SA and Gullick WJ (1994). Identification of c-erbB-3 binding sites for phosphatidylinositol 3′-kinase and SHC using an EGF receptor/c-erbB-3 chimera. *EMBO J* **13**, 2831–2841.

[17] Manning BD and Cantley LC (2007). AKT/PKB signaling: navigating downstream. *Cell* **129**, 1261–1274.

[18] Baselga J and Swain SM (2009). Novel anticancer targets: revisiting ERBB2 and discovering ERBB3. *Nat Rev Cancer* **9**, 463–475.

[19] Aurisicchio L, Marra E, Roscilli G, Mancini R, and Ciliberto G (2012). The promise of anti-ErbB3 monoclonals as new cancer therapeutics. *Oncotarget* **3**, 744–758.

[20] Lazrek Y, Dubreuil O, Garambois V, Gaborit N, Larbouret C, Le Clorennec C, Thomas G, Leconet W, Jarlier M, Pugnière M, et al. (2013). Anti-HER3 domain 1 and 3 antibodies reduce tumor growth by hindering HER2/HER3 dimerization and AKT-induced MDM2, XIAP, and FoxO1 phosphorylation. *Neoplasia* **15**, 335–347.

[21] Lorusso P, Jänne PA, Oliveira M, Rizvi N, Malburg L, Keedy V, Yee L, Copigneaux C, Hettmann T, Wu CY, et al. (2013). Phase I study of U3-1287, a fully human anti-HER3 monoclonal antibody, in patients with advanced solid tumors. *Clin Cancer Res* **19**, 3078–3087.

[22] Sala G, Traini S, D'Egidio M, Vianale G, Rossi C, Piccolo E, Lattanzio R, Piantelli M, Tinari N, Natali PG, et al. (2012). An ErbB-3 antibody, MP-RM-1, inhibits tumor growth by blocking ligand-dependent and independent activation of ErbB-3/Akt signaling. *Oncogene* **31**, 1275–1286.

[23] Petronzelli F, Pelliccia A, Anastasi AM, D'Alessio V, Albertoni C, Rosi A, Leoni B, De Angelis C, Paganelli G, Palombo G, et al. (2005). Improved tumor targeting by combined use of two antitenascin antibodies. *Clin Cancer Res* **11**, 7137s–7145s.

[24] Leonetti C, D'Agnano I, Lozupone F, Valentini A, Geiser T, Zon G, Calabretta B, Citro GC, and Zupi G (1996). Antitumor effect of c-myc antisense phosphorothioate oligodeoxynucleotides on human melanoma cells *in vitro* and in mice. *J Natl Cancer Inst* **88**, 419–429.

[25] Rege-Cambrin G, Scaravaglio P, Carozzi F, Giordano S, Ponzetto C, Comoglio PM, and Saglio G (1992). Karyotypic analysis of gastric carcinoma cell lines carrying an amplified c-met oncogene. *Cancer Genet Cytogenet* **64**, 170–173.

[26] Sala G, Dituri F, Raimondi C, Previdi S, Maffucci T, Mazzoletti M, Rossi C, Iezzi M, Lattanzio R, Piantelli M, et al. (2008). Phospholipase Cγ1 is required for metastasis development and progression. *Cancer Res* **68**, 10187–10196.

[27] Li N, Hill KS, and Elferink LA (2008). Analysis of receptor tyrosine kinase internalization using flow cytometry. *Methods Mol Biol* **457**, 305–317.

[28] Arai K, Yoshinari K, Matsumoto K, and Misaki H (1998). An ELISA to determine the biodistribution of human monoclonal antibody in tumor-xenografted SCID mice. *J Immunol Methods* **217**, 79–85.

[29] Jaiswal BS, Kljavin NM, Stawiski EW, Chan E, Parikh C, Durinck S, Chaudhuri S, Pujara K, Guillory J, Edgar KA, et al. (2013). Oncogenic ERBB3 mutations in human cancers. *Cancer Cell* **23**, 603–617.

[30] Engelman JA, Zejnullahu K, Mitsudomi T, Song Y, Hyland C, Park JO, Lindeman N, Gale CM, Zhao X, Christensen J, et al. (2007). MET amplification leads to gefitinib resistance in lung cancer by activating ERBB3 signaling. *Science* **316**, 1039–1043.

[31] Sergina NV, Rausch M, Wang D, Blair J, Hann B, Shokat KM, and Moasser MM (2007). Escape from HER-family tyrosine kinase inhibitor therapy by the kinase-inactive HER3. *Nature* **445**, 437–441.

[32] Chakrabarty A, Sanchez V, Kuba MG, Rinehart C, and Arteaga CL (2012). Feedback upregulation of HER3 (ErbB3) expression and activity attenuates antitumor effect of PI3K inhibitors. *Proc Natl Acad Sci USA* **109**, 2718–2723.

[33] Garrett JT, Olivares MG, Rinehart C, Granja-Ingram ND, Sánchez V, Chakrabarty A, Dave B, Cook RS, Pao W, McKinely E, et al. (2011). Transcriptional and posttranslational up-regulation of HER3 (ErbB3) compensates for inhibition of the HER2 tyrosine kinase. *Proc Natl Acad Sci USA* **108**, 5021–5026.

[34] Abel EV, Basile KJ, Kugel CH, Witkiewicz AK, Le K, Amaravadi RK, Karakousis GC, Xu X, Xu W, Schuchter LM, et al. (2013). Melanoma adapts to RAF/MEK inhibitors through FOXD3-mediated upregulation of ERBB3. *J Clin Invest* **123**, 2155–2168.

[35] Vaswani SK and Hamilton RG (1998). Humanized antibodies as potential therapeutic drugs. *Ann Allergy Asthma Immunol* **81**, 105–115; quiz 115-106, 119.

[36] Kipriyanov SM and Little M (1999). Generation of recombinant antibodies. *Mol Biotechnol* **12**, 173–201.

[37] Sievers EL and Senter PD (2012). Antibody-drug conjugates in cancer therapy. *Annu Rev Med* **64**, 15–29.